Published in final edited form as:
Acta Biomater. 2015 January 15; 12: 21–29. doi:10.1016/j.actbio.2014.10.030.

Phenotypic Stability, Matrix Elaboration, and Functional Maturation of Nucleus Pulposus Cells Encapsulated in Photocrosslinkable Hyaluronic Acid Hydrogels

Dong Hwa Kim[a,b], **John T. Martin**[a,b,c], **Dawn M. Elliott**[d], **Lachlan J. Smith**[a,b,e], and **Robert L. Mauck**[a,b,c,f,*]

[a]Department of Orthopaedic Surgery, University of Pennsylvania, McKay Orthopaedic Research Laboratory, 36th Street and Hamilton Walk, 424 Stemmler Hall, Philadelphia, PA 19104-6081, USA

[b]Translational Musculoskeletal Research Center, Philadelphia VA Medical Center, 3900 Woodland Avenue, Building 21, Room A200, Philadelphia, PA 19104, USA

[c]Department of Mechanical Engineering and Applied Mechanics, University of Pennsylvania, 220 South 33rd Street, 229 Towne Building, Philadelphia, PA 19104-6315, USA

[d]Department of Biomedical Engineering, University of Delaware, 125 E. Delaware Avenue, Newark, DE 19716, USA

[e]Department of Neurosurgery, University of Pennsylvania, 3400 Spruce Street, 3rd Floor, Silverstein Pavilion, Philadelphia, PA 19104, USA

[f]Department of Bioengineering, University of Pennsylvania, 210 South 33rd Street, Suite 240, Skirkanich Hall, Philadelphia, PA 19104-6321, USA

Abstract

Degradation of the nucleus pulposus (NP) is an early hallmark of intervertebral disc degeneration. The capacity for endogenous regeneration in the NP is limited due to the low cellularity and poor nutrient supply of this avascular tissue. Towards restoring the NP, a number of biomaterials have been explored for cell delivery. These materials must support the NP cell phenotype while promoting the elaboration of an NP-like extracellular matrix in the shortest possible time. Our previous work with chondrocytes and mesenchymal stem cells demonstrated that hydrogels based on hyaluronic acid (HA) are effective at promoting matrix production and the development of functional material properties. However, this material has not been evaluated in the context of NP cells. Therefore, to test this material for NP regeneration, bovine NP cells were encapsulated in 1% w/vol HA hydrogels at either a low seeding density (20×10^6 cells/ml) or a high seeding

Corresponding Author: Robert L. Mauck, PhD, Associate Professor of Orthopaedic Surgery and Bioengineering, McKay Orthopaedic Research Laboratory, University of Pennsylvania, 424 Stemmler Hall, 36th Street and Hamilton Walk, Philadelphia, PA 19104, Phone: 215-898-3294, Fax :215-573-2133, lemauck@mail.med.upenn.edu.

density (60×10^6 cells/ml), and constructs were cultured over an 8 week period. These engineered NP cell-laden HA hydrogels showed functional matrix accumulation, with increasing matrix content and mechanical properties with time in culture at both seeding densities. Furthermore, encapsulated cells showed NP-specific gene expression profiles that were significantly higher than expanded NP cells prior to encapsulation, suggesting a restoration of phenotype. Interestingly, these levels were higher at the lower seeding density compared to the higher seeding density. These findings support the use of HA-based hydrogels for NP tissue engineering and cellular therapies directed at restoration or replacement of the endogenous NP.

Keywords

Intervertebral disc degeneration; cell therapy; three-dimensional culture; mechanical properties; tissue engineering

1. Introduction

Degeneration of lumbar intervertebral discs is strongly implicated as a cause of low back pain [1]. The central nucleus pulposus (NP) is critical for the mechanical function of the disc. The NP is a proteoglycan-rich gelatinous structure in the central region of the disc that is constrained circumferentially by the tough, fiber-reinforced annulus fibrosus (AF). When axial loads are applied to the spinal motion segment (bone-disc-bone unit), the NP is constrained from expanding by the AF, and so instead pressurizes, enabling even load transfer between adjacent vertebral bodies. Changes to the NP are an early hallmark of disc degeneration [2,3], and involve concurrent decreases in cell density, increases in inflammatory factors, fibrotic changes in tissue structure, and an overall reduction in the synthesis of NP-specific extracellular matrix (ECM), especially proteoglycans [4]. During degeneration, this loss of NP-specific matrix content impairs NP mechanical function, decreasing swelling capacity and pressurization potential [5]. After the onset of degeneration, endogenous repair is limited due to the low cell density and poor nutrient supply of this avascular tissue [6].

Current treatments for disc degeneration, both conservative and surgical, have limited efficacy [7], and so there has been a strong focus on development of new, biologic-based therapies that can restore and maintain native disc structure and mechanical function. To this end, tissue engineering efforts have sought to develop substitutes for the degenerated NP. Hydrogels in particular are among the most widely considered scaffold materials for NP tissue engineering as the native NP is a loosely crosslinked water swollen network (~90% water by weight), very similar in composition to many hydrogels used in biomedical applications [8]. Hydrogels for NP applications can either be used in an acellular form, including novel formulations that are ‘PGrich’ by design [9], or in combination with cells [8,10]. Importantly, hydrogel delivery can be performed minimally-invasively (i.e., percutaneously), and some formulations have been shown to restore aspects of native tissue composition and function in early translational studies [11]. A number of natural biopolymers have been considered for cell-based NP tissue engineering applications, including agarose [12,13], alginates that are both ionically and covalently crosslinked [10],

carboxymethylcellulose [14], fibrin/fibrinogen [15], chitosan [16], and combinations thereof [17]. When encapsulated in these materials, NP and progenitor cells (i.e. mesenchymal stem cells) express NP-specific markers and accumulate NP-like ECM, including type II collagen and proteoglycans [13,18,19]. However, only a few studies have interrogated the mechanical properties of these constructs as a function of culture duration. For example, we recently showed that NP cells seeded in agarose can establish a functional NP-like material in vitro [13]. While promising, the translational potential and long term efficacy of agarose may be limited by its inability to degrade and be replaced by native tissue.

Over the last decade, we have explored the use of methacrylated hyaluronic acid (HA) as a cell carrier and hydrogel for the engineering of cartilaginous tissues using a variety of cell types, including chondrocytes and mesenchymal stem cells (MSCs) [20]. This material, when coupled with a photo-initiator, can form stable hydrogels upon UV exposure. Importantly, HA is used in many FDA approved clinical procedures, and is biodegradable, increasing its translational potential [21,22]. Moreover, HA plays a critical role in the biology of the native NP matrix, where long chains of HA act as backbones for aggregating proteoglycans, contributing to the development of a functional extracellular matrix, while also evoking a positive biological effect on ECM production, cell migration, and phenotypic maintenance of chondrocytes and NP cells [23]. When chondrocytes or MSCs are cultured in HA hydrogels under pro-chondrogenic conditions, these hydrogel constructs increase in mechanical functionality and ECM content with time [24]. More recently, we have shown that specific biologic interactions that cells have with HA via the CD44 receptor promote the early commitment of progenitor cells to the chondrogenic lineage, with associated positive effects on for functional ECM deposition [25]. HA has also been used in combination with other materials to create composite hydrogels to take advantage of this biologic functionality. For example, Collin et al. developed an injectable type II collagen/HA hydrogel that promoted cell viability [26] while Park et al. fabricated a fibrin/HA/silk composite gels that increased expression of type II collagen, sox9, and aggrecan, and maintained mechanical integrity *in vitro* [27]. Still more recently, Peroglio et al. developed a set of hyaluronan-based thermoreversible hydrogels (HA-pNIPAM) to serve as NP cell carriers, and cultured these cell laden constructs for 1 week, with comparisons made to alginate gel beads. These HA-pNIPAM hydrogels maintained the NP cell phenotype and promoted ECM production [28].

In order to translate HA-based materials towards *in vivo* applications, it is important to consider the cell density and material attributes that will most effectively generate an NP-like tissue in the shortest possible time. One approach to improving the functional maturation of an NP cell-based engineered construct may be to increase the initial cell density within the construct. In the adult, the NP is matrix-rich, and cell poor, with a small number of endogenous cells (only ~ 6000 cells per mm3, equating to ~6 million cells per mL). It is widely accepted that this low cell density is all that can be supported by the poor nutritional supply to the NP space [6]. However, during development, the NP begins essentially as a cell-rich, matrix poor aggregation (i.e., its entirety is composed of cells prior to matrix deposition). A similar transition occurs in articular cartilage, where for example in fetal cartilage the cell density is as high as 100 million cells/mL, dropping to ~10 million

cells/mL in the adult [29]. In both tissues, the high cellularity of the fetal state is thought to be required for the rapid accumulation and assembly of extracellular matrix, as well as its ability to repair itself. Indeed, this thinking informs many of our tissue engineering approaches, where for example increasing the seeding density of the engineered construct can improve growth trajectories [30]. Using the same seeding densities as were employed here (20 and 60 million cells per ml) with bovine mesenchymal stem cells in HA hydrogels (for cartilage tissue engineering purposes), higher cell densities resulted in improved functional outcomes with long term culture [24]. While these data point to a more rapid formation of an engineered construct for other cell types, this had not previously been assayed with NP cells in this HA system.

To that end, the objective of this study was to determine whether increasing the seeding density of NP cells in an HA hydrogel would enhance construct maturation. NP cells were seeded in 1% w/vol macromer density HA hydrogels at either 20×10^6 or 60×10^6 cells/ml, and cultured over an 8 week period in a chemically defined medium formulation. At multiple time points, construct maturation was evaluated by assessment of the biomechanical properties, expression of NP-specific genes, biochemical composition, and ECM distribution to determine the appropriate NP seeding density for this HA-based NP tissue engineering system.

2. Materials and Methods

2.1. Fabrication of Hyaluronic Acid (HA) Hydrogels

Methacrylated HA (MeHA) was produced by reacting 65 kDa HA (Lifecore; Chaska, MN, USA) with methacrylic anhydride (Sigma Aldrich; St. Louis, MO, USA) as previously described [21]. The degree of methacrylation was ~25%, as assessed by 1H-NMR as previously described [21]. Lyophilized MeHA was sterilized by exposure to a biocidal UV light for 15 min. Prior to cell encapsulation, the macromer was dissolved at 1% w/vol in sterile phosphate-buffered saline with addition of 0.05% w/vol of the photoinitiator, Irgacure 2959 (2-methyl-1-[4-(hydroxyethoxy)phenyl]-2-methyl-1-propanone; Ciba-Geigy; Tarrytown, NY, USA).

2.2. Nucleus Pulposus Cell Isolation, Expansion, and 3D Culture

NP tissue was isolated from four adult bovine caudal discs, purchased from a local slaughterhouse, according to institutional guidelines. NP cells (NPCs) were isolated from dissected tissue via digestion for 1 hour in 2.5 mg/mL pronase, followed by 4 hours in 0.5 mg/mL collagenase at 37°C. After digestion, the cell suspension was filtered through a 70 μm strainer. Isolated NPCs were expanded in high-glucose DMEM containing 10% fetal bovine serum (FBS) and 1% PSF. Passage 2 cells from all donor animals were combined and seeded into 1% w/vol MeHA solutions at a densities of either 20 million cells/ml (20M) or 60 million cells/ml (60M) as described previously [24].

NPC-laden MeHA macromer suspensions were then cast between glass plates separated by a 1.5 mm spacer, and photo-polymerized with UV exposure for 10 minutes. Constructs were then formed from gel slabs using a 4 mm biopsy punch, and cultured in chemically defined

medium (1mL/construct) comprised of high-glucose DMEM supplemented with 1% PSF, 0.1 μM dexamethasone, 50 mg/mL ascorbate 2-phosphate, 40 mg/mL L-proline, 100 mg/mL sodium pyruvate, and ITS Premix (6.25 μg/mL insulin, 6.25 μg/mL transferrin, 6.25 ng/mL selenous acid), 1.25 mg/mL bovine serum albumin (BSA), 5.35 μg/mL linoleic acid). Media was further supplemented with TGF-β3 (10 ng/mL; R&D Systems; Minneapolis, MN, USA) and constructs were cultured for up to 8 weeks. Media were changes three times weekly, with the last change (representing culture for 3 days) collected for analysis of media composition.

2.3. Mechanical Testing

Unconfined compression tests were performed on days 1, 28 and 56 using a custom mechanical testing device [31] to determine construct mechanical properties as a function of time and seeding density. Sample dimensions were measured with a digital caliper and testing took place in a PBS bath. Initially, for each construct a constant 2 g load was applied and creep displacement was monitored until equilibrium was attained (~300s). Subsequently, a stress relaxation test a was carried out via a single compressive deformation to 10% strain at a rate of 0.05% per second followed by 20 min of relaxation to equilibrium, at which point stress and strain values were used to calculate the equilibrium modulus. Dynamic mechanical properties were evaluated after equilibrium via the application of a 1% sinusoidal deformation at 1 Hz for 10 cycles. The dynamic modulus was calculated from the dynamic stress-strain curve. After testing, constructs were frozen at −20°C for subsequent biochemical evaluation.

2.4. Cell Morphology and Viability

To evaluate NPC morphology and viability as a function of culture duration, constructs were imaged using a Live/Dead staining kit (Molecular Probes; Eugene, OR, USA). Constructs were halved across the midline, rinsed twice with PBS, and incubated for 30 min at room temperature with 2 μM Calcein AM and 4 μM ethidium homodimer-1. The central regions of constructs were imaged using a confocal microscope (LSM 510; Carl Zeiss; Oberkochen, Germany) at 20× magnification. Analysis took place on days 1, 7, 14, 28 and 56. Quantification of total cell number and viable cell fraction were determined from the live/dead images using the cell counter function in Image J (National Institutes of Health; Bethesda, MD, USA).

2.5. Biochemical Composition

After mechanical testing, samples were weighed and digested overnight in papain [32]. Sulfated glycosaminoglycan (s-GAG), and collagen content were assessed on days 1, 28 and 56 as previously described [32]. Briefly, s-GAG content was determined using the 1, 9-dimethylmethylene blue (DMMB) dye binding assay with chondroitin-6 sulfate as a standard, respectively. s-GAG released to the culture medium was also measured using the DMMB assay, and is reported as s-GAG released per day of culture. Digested samples were then hydrolyzed overnight in 6M HCl at 110 °C and collagen content determined using the orthohydroxyproline (OHP) assay [33], assuming a ratio of OHP to collagen of 1:7.14 [34]. Construct sGAG and collagen contents are reported normalized per construct and per construct wet weight.

2.6. Histological Analysis of Matrix Distribution

Constructs were fixed in 4% paraformaldehyde, infiltrated with Citrisolv, embedded in paraffin, and sectioned (to 8 μm thickness) on days 1, 28 and 56. Samples were stained with either Alcian blue or Picrosirius Red to visualize proteoglycans and collagens, respectively, as previously described [35]. For immunohistochemical detection of collagen type II, sections were incubated in proteinase K at room temperature for 4 mins followed by blocking with 10% NGS for 30 mins at RT. Primary antibody (collagen type II, 11-116B3, Developmental Studies Hybridoma Bank; Iowa City, IA, USA) was applied at a concentration of 10 μg/mL at 4°C overnight, followed by a one hour incubation with secondary antibody at RT. Staining was visualized using DAB chromagen reagent (DAB150 IHC Select; EMD Millipore; Bellirica, MA, USA) according to the manufacturer's protocol. Staining was visualized and imaged under bright field microscopy.

2.7. Gene Expression

Messenger RNA was isolated from NP constructs and expanded and freshly isolated NP cells using the TRIzol/chloroform method [36], and quantified using a spectrophotometer (ND-1000; Nanodrop Technologies, Wilmington, DE, USA). Reverse transcription was carried out with random hexamers using the Superscript II Kit (ThermoFisher Scientific; Waltham, MA, USA). Real time RT-PCR was performed on an Applied Biosystems Step-One System and with SYBR Green Master Mix (ThermoFisher Scientific) to determine expression levels of aggrecan (ACAN), collagen II (COL2A1), SOX9, collagen I (COL1A2), as well as the NPC specific markers cytokeratins (KRT) 8, 18, 19, and N-cadherin (CDH 2) after 28 and 56 day of culture. Expression levels were normalized to glyceraldehyde 3-phosphate dehydrogenase (GAPDH) and compared to levels in expanded NPCs prior to encapsulation as well as freshly isolated NP cells. Primer sequences are provided in Table 1.

2.8. Statistical Analysis

Statistical analyses were performed by a 2 way analysis of variance (ANOVA) using a SYSTAT 10.3 (Systat Software; Point Richmond, CA, USA). All results are expressed as mean ± standard deviation. Significance was set at $p \leq 0.05$, with comparisons between groups carried out using Fisher's least significant difference (LSD) post hoc testing.

3. Results

3.1. Cell Morphology and Viability

NPC-seeded HA constructs were successfully formed at densities of 60M or 20M. As early as day 14, NPCs adopted a non-spherical morphology at the lower seeding density (20M), while they formed small clusters of spherical cells at the higher seeding density (60M). By day 56, both seeding densities had a non-spherical morphology (Fig. 1A). At day 1, the total number of cells in the 60M seeding group was ~2.4-fold higher than for the 20M seeding group ($p < 0.05$, Fig. 1B). Total cell number decreased with culture time for the 60M group, but no significant changes were observed for the 20M group (Fig. 1B). There were no differences in viability between 60M and 20M constructs at any time point (Fig. 1C).

3.2. Biochemical Composition and ECM Distribution

Construct wet weight was not significantly different between 60M and 20M groups at any time point, and the wet weight significantly increased by day 56 (Fig. 2A). GAG content increased over the culture period in both 60M and 20M groups ($p < 0.05$), with only minor differences between groups. On day 56, total GAG content per construct reached 1300 μg and 1100 μg in 60M and 20M constructs, respectively, with no significant difference between groups (Fig. 2B). On day 56, both 20M and 60M groups had GAG contents reaching over 3% of construct wet weight (Fig. 2C). GAG released into the media per day was relatively low over the first 21 days culture, and not significantly different between groups. Between days 21 and 28, however, there was a significant increase (~3 fold) in GAG release, reaching a new equilibrium level that again was not different between groups (Fig. 2D). Similar to GAG results, collagen content increased over the culture period, with only minor differences between groups. Total collagen content per construct reached ~ 400 μg in 60M and 20M constructs on day 56, with no significant difference between groups (Fig. 2E). Collagen content on day 56 was ~1% of wet weight for both groups (Fig. 2F).

Histological staining of constructs was generally consistent with biochemical measures. Alcian blue staining intensity increased substantially in all constructs with culture duration, with slightly more intense staining in 60M constructs at both day 28 and day 56 (Fig. 3A). Picrosirius red staining of collagen likewise showed a gradual accumulation of collagen in both 60M and 20M constructs with culture duration (Fig. 3B). Type II collagen was uniformly distributed (Fig. 3C).

3.3. Mechanical Properties

Constructs increased in equilibrium and dynamic modulus with time in culture. On day 28, the equilibrium modulus of 60M constructs was 2 times greater than 20M constructs ($P < 0.05$). However, by day 56, both seeding densities showed further improvements in properties and the 60M constructs were no longer different than 20M constructs. At this time point, both groups had reached an equilibrium modulus in excess of 150 kPa (Fig. 4A). The dynamic compressive modulus likewise increased with time in culture, though there were no differences between 60M and 20M constructs at any time point ($p > 0.05$). On day 56, the dynamic modulus reached 1.5–2.0 MPa for both groups (Fig. 4B).

3.4. Gene Expression

Gene expression analysis was carried out to determine whether NPCs encapsulated in HA hydrogels were capable of re-expressing markers of the NP phenotype. In 60M constructs, ACAN expression was 8 and 38 fold higher than that of expanded NPCs prior to encapsulation at days 28 and 56 ($p < 0.05$, Fig. 5A), respectively. In 20M constructs, ACAN was 16 and 32 fold higher on days 28 and 56, respectively (not significantly different). COL2A1 expression in 60M constructs increased 9 and 35 fold compared to NPCs prior to encapsulation on days 28 and 56 ($p < 0.05$) respectively. In 20M constructs, COL2A1 increased 17 and 28 fold on days 28 and 56, respectively (not significantly different). There was no significant difference in the level of SOX9 expression in either 60M or 20M constructs compared to NPCs prior to encapsulation at day 28. However, at day 56, SOX9 expression in both 60M and 20M constructs was 2 times higher than expanded NPC levels

($p < 0.05$). Expression of COL1A2 was down-regulated in 60M constructs ($p < 0.05$); COL1A2 in 20M constructs was 0.6 times that of control on day 28, but was not different from expanded NPCs on day 56. Expression of the NPC specific markers KRT18 and CDH2 did not change in either the 60M or 20M constructs during the culture period ($p > 0.05$). Expression of KRT8 was not different from expanded NPCs on day 28 ($p > 0.05$), but levels were 5 and 10 fold higher than in expanded NPCs on day 56 for 60M and 20M constructs ($p < 0.05$). KRT19 was upregulated in both 60M and 20M constructs ($p < 0.05$); on day 28, expression was 9 and 18 fold higher than expanded NPC, respectively ($p < 0.05$). Between days 28 and 56, KRT19 expression in 60M constructs slightly increased ($p > 0.05$), while expression in 20M constructs significantly increased ($p < 0.05$).

Expression of all NPC-specific markers, including KRT8, KRT18, KRT19 and CDH2, was significantly higher in 20M constructs compared to 60M constructs on day 56 ($p < 0.05$). Expression levels in constructs were also compared to freshly isolated NP cells (Fig. 5B). ACAN expression at day 28 for 60M and 20M constructs was 11% and 25% that of freshly isolated cells ($p < 0.05$, Fig. 5B). At day 56, ACAN expression for 60M constructs was 82% of that of freshly isolated cells ($p > 0.05$), while for 20M constructs it was significantly lower. Expression of COL2A1 was lower for both seeding densities and at both time points compared to freshly isolated levels, though differences were not significant. Expression of SOX9 at day 28 for 60M and 20M constructs was 22% and 32% that of freshly isolated NP cells (both $p < 0.05$), 44% in 60M after 56 days ($p < 0.05$) and 77% in 20M after 56 days ($p > 0.05$). COL1A2 expression at day 28 for 60M and 20M constructs was 2-fold and 5.6-fold that of freshly isolated cells ($p > 0.05$), 6.8-fold in 60M after 56 days, and 5.7-fold in 20M after 56 days (none significantly different). Expression of NPC-specific markers, (KRT8, KRT18, KRT19 and CDH2), was all significantly lower for both 60M and 20M constructs compared to freshly isolated cells at both time points.

4. Discussion

In this study, we investigated the functional maturation of constructs formed from NPCs in an HA hydrogel, and the appropriate NPC seeding density to maximize construct maturation. NPC-laden HA hydrogels showed functional matrix accumulation, with GAG and collagen contents after 8 weeks of culture similar for both initial seeding densities. Furthermore, mRNA expression of NPC specific markers, together with important extracellular matrix molecules aggrecan and collagen II, increased significantly with time in culture, suggesting that the HA hydrogel promoted restoration and maintenance of the native NPC phenotype.

Previous studies have shown that NPCs lose their phenotypic characteristics when cultured in monolayer, with the expression of type II collagen and aggrecan mRNA reduced with serial passaging [37]. In this study, when NPCs were cultured in HA hydrogels, COL1A2 gene expression was down-regulated while ACAN and COL2A1 expression levels increased relative to expanded NP cells at the beginning of HA culture. This suggests that the HA hydrogel is an appropriate 3D culture environment for supporting the restoration of the native NPC phenotype following monolayer expansion [26]. SOX9 is a master regulator of the chondrocyte phenotype [38] and is involved in the control of collagen type II activation

and synthesis [39]. In this study, we found that hydrogel-encapsulated NPCs expressed higher levels of SOX9 mRNA than NPCs cultured in monolayer. In addition to these markers that are also involved in cartilage tissue formation, recent studies have identified a number of additional molecules that can distinguish NPCs from articular chondrocytes [40–42], including KRT18, neural cell adhesion molecule, glypican-3, and KRT19. Indeed, the markers KRT8, 18, and 19 are differentially expressed in mature NPCs compared to articular cartilage chondrocytes and AF cells [43,44]. Comparison of gene expression in human disc cells and articular cartilage cells provided strong evidence that KRT19 might be a positive marker for NP-like cells in comparison to other potential markers [42,44]. KRT19 is an intermediate filament expressed in notochordal cells, and other tissues during embryonic development [45]. In the current study, expression of KRT8 and KRT19 increased significantly in HA constructs. Interestingly, these NP-specific markers were significantly higher in low seeding density (20M) constructs compared to high seeding density (60M) constructs on day 56. This is the first report that demonstrates upregulation of KRT8 and KRT19 in HA-cultured NPCs, indicating that our model may promote redifferentiation of these cells towards an NPC like phenotype. The mRNA expression levels of NP cell markers were also compared to those of freshly isolated NPCs. For some markers including ACAN, COL2A1 and SOX9, expression approached native tissue levels, while other markers (KRT8, 18, 19 and CHD2) continued to be expressed at a small fraction of native levels. These results support the conclusion that culture of NPCs in HA promotes the elaboration of an appropriate extracellular matrix. The consequences of ineffective restoration of these other NP-specific markers is unclear, as the functions of these molecules remains poorly understood. It is likely that additional physical or biochemical cues will be necessary to induce their expression.

This study employed a modified version of the natural ECM constituent HA to form a stable, covalently cross-linked hydrogel [24]. HA forms a structural component in all cartilaginous extracellular matrices, and interacts with specific cell surface receptors to promote cell adhesion and migration. An added benefit of the HA system is that material density can be readily altered and additional functionalities can be superimposed upon this template via straightforward modification of the HA backbone. For instance, we recently showed that appending ligands such as RGD and N-Cadherin to the HA backbone alters MSC differentiation and biosynthesis [25]. In previous studies, a composite hydrogel of HA and collagen II improved NPC phenotypic maintenance [46], and studies with HA-enriched collagen II hydrogels suggested that HA can improve mechanical properties [47]. In this study, we found that NP cells survived, proliferated and aggregated to form clusters when encapsulated in HA hydrogels. Interestingly, cells cultured at low seeding density (20M) showed differences compared with higher seeding density (60M) early in culture. Specifically, NPCs adopted a non-spherical morphology at the lower seeding density, while they formed small clusters of spherical cells at the higher seeding density. Peroglio et al. cultured NPCs (3×10^6 cells/mL) within 10% w/v HA- pNIPAM 20 and 35 solutions for 1 week. The characteristic rounded morphology of NPCs was maintained in the HA- pNIPAM 20 hydrogel. However, NPCs in HA-pNIPAM 35 hydrogel lost their rounded shape and elongated, and the gels shrunk by ~30%. Thus, NPCs might adopt different morphologies depending on construct volume changes, seeding density, concentration of HA [28].

The ability of NPCs to remodel their material microenvironment is particularly relevant when considering the ultimate biochemical and biomechanical functionality of the construct. Interestingly, this study showed marked increases in properties at both seeding densities. While the higher seeding density led to a more rapid increase in properties (with differences apparent at day 28), by day 56 the properties were not different from one another, with 20M constructs reaching a modulus of 166 kPa, and the 60M reached 169 kPa. Furthermore, sGAG content reached comparable levels between the two groups. GAG and collagen comprise around 4.7% and 3.9% of native bovine NP by wet weight respectively [13], suggesting that our NPC-laden HA hydrogels achieved approximately 75% of native GAG content and 32% of native collagen content. In a previous study using MSCs in this material, the equilibrium modulus achieved was ~3-fold greater at 60 vs 20M seeding density, while the sGAG content was only ~25% greater [24]. This suggests a divergent behavior between MSCs and NPCs on this hydrogel platform. At low densities, NPCs may have better access to nutrients, which consequently increases the efficiency with which they can produce ECM. Conversely, the higher cell density may have led to decreases in nutrient supply, including oxygen and glucose [48]. For example, Kobayashi et al. examined two initial seeding NPC and chondrocyte densities (4–5 million cells/ml and 25 million cells/ml) in alginate beads over 5 days. They showed that cells cultured at low density were more active and accumulated significantly more GAG per cell than cells cultured at high density [49]. The chemical, mechanical and histological analyses performed here and elsewhere imply that the outcomes of engineered NP constructs do depend on the initial seeding density, and further suggest that this should be carefully controlled when transitioning this technology to the nutrient poor *in vivo* environment of the disc, where the delivery of too many cells may result in a counter-productive outcome.

Taken together, our findings suggest that a lower initial NPC seeding density (20×10^6 cells/mL) is sufficient for engineering NP-like tissues with HA hydrogels. This has clinical relevance, as the supply of autologous NPCs is limited, and culture expansion of such cells may limit the retention of their phenotype. Having established that this crosslinkable HA material is supportive of the formation of an NP-like tissue and resumption of an NPC-like phenotype, current work is focused on implementing other gelation mechanisms that would enable injectable delivery of this material to the disc space (i.e., redox-mediated reactions [50]). Further, we are employing this material in conjunction with a nanofiber-based annulus fibrosus replacement [12], to generate entire whole disc constructs for direct implantation [51]. Ultimately, these NP-like engineered materials may provide a framework for restoring function in the degenerated intervertebral disc.

5. Conclusion

In this study, we investigated the functional maturation of constructs formed from NPCs in HA hydrogels, and the appropriate NPC seeding density to enhance construct maturation. We found functional matrix accumulation in NPC-laden HA hydrogels, with GAG and collagen content reaching comparable levels, independent of the initial seeding density. Furthermore, it was demonstrated that expression of NP specific markers (including KRT8 and KRT19), together with the important extracellular matrix molecules aggrecan and collagen II, increased significantly with time in culture, suggesting that this material

supports the resumption of the NPC phenotype following culture expansion. Future work will employ these NPC-laden HA hydrogels in conjunction with a nanofiber-based annulus fibrosus replacement for tissue engineered total disc replacement.

Acknowledgements

This work was supported by the Department of Defense (Grant OR090090), the Department of Veterans Affairs (Grant I01 RX000211), and the Penn Center for Musculoskeletal Disorders (Grant P30 AR050950).

References

1. Bogduk N. The lumbar disc and low back pain. Neurosurg Clin N Am. 1991; 2:791–806. [PubMed: 1821758]
2. Jensen M, Kelly A, Brant-Zawadzki M. MRI of degenerative disease of the lumbar spine. Magn Reson Q. 1994; 10:173–190. [PubMed: 7811610]
3. Kestle JRW, Resch L, Tator CH, Kucharczyk W. Intervertebral disc embolization resulting in spinal cord infarction. J Neurosurg. 1989; 71:938–941. [PubMed: 2585089]
4. Huang B, Zhuang Y, Li CQ, Liu LT, Zhou Y. Regeneration of the intervertebral disc with nucleus pulposus cell-seeded collagen II/hyaluronan/chondroitin-6-sulfate tri-copolymer constructs in a rabbit disc degeneration model. Spine (Phila Pa 1976). 2011; 36(26):2252–2259. [PubMed: 21358466]
5. Cortes DH, Jacobs NT, DeLucca JF, Elliott DM. Elastic, permeability and swelling properties of human intervertebral disc tissues: A benchmark for tissue engineering. J Biomech. 2014; 47(9): 2088–2094. [PubMed: 24438768]
6. Maroudas A, Stockwell RA, Nachemson A, Urban J. Factors involved in the nutrition of the human lumbar intervertebral disc: cellularity and diffusion of glucose in vitro. J. Anat. 1975; 120(1):113–130. [PubMed: 1184452]
7. An H, Boden SD, Kang J, Sandhu HS, Abdu W, Weinstein J. Summary statement: emerging techniques for treatment of degenerative lumbar disc disease. Spine. 2003; 28(15)):S24–S25. [PubMed: 12897470]
8. Cloyd JM, Malhotra NR, Weng L, Chen W, Mauck RL, Elliott DM. Material properties in unconfined compression of human nucleus pulposus, injectable hyaluronic acid-based hydrogels and tissue engineering scaffolds. Eur Spine J. 2007; 16(11):1892–1898. [PubMed: 17661094]
9. Calderon L, Collin E, Velasco-Bayon D, Murphy M, O'Halloran D, Pandit A. Type II collagen-hyaluronan hydrogel – a step towards a scaffold for intervertebral disc tissue engineering. Eur Cell Mater. 2010; 20:134–148. [PubMed: 20821371]
10. Chou AI, Nicoll SB. Characterization of photocrosslinked alginate hydrogels for nucleus pulposus cell encapsulation. J of Biomed Mater Res Part A. 2009; 91A(1):187–194.
11. Malhotra NR, Han WM, Beckstein J, Cloyd J, Chen W, Elliott DM. An Injectable Nucleus Pulposus Implant Restores Compressive Range of Motion in the Ovine Disc. Spine. 2012; 37(18):E1099–E1105. [PubMed: 22588378]
12. Nerurkar NL, Sen S, Huang AH, Elliott DM, Mauck RL. Engineered disc-like angle-ply structures for intervertebral disc replacement. Spine (Phila Pa 1976). 2010; 35(8):867–873. [PubMed: 20354467]
13. Smith LJ, Chiaro JA, Nerurkar NL, Cortes DH, Horava SD, Hebela NM, et al. Nucleus pulposus cells synthesize a functional extracellular matrix and respond to inflammatory cytokine challenge following long term agarose culture. Eur Cell Mater. 2012; 22:291–301. [PubMed: 22102324]
14. Reza AT, Nicoll SB. Characterization of novel photocrosslinked carboxymethylcellulose hydrogels for encapsulation of nucleus pulposus cells. Acta Biomater. 2010; 6(1):179–186. [PubMed: 19505596]
15. Perka C, Arnold U, Spitzer R-S, Lindenhayn K. The use of fibrin beads for tissue engineering and subsequential transplantation. Tissue Eng. 2001; 7:359–361. [PubMed: 11429155]

16. Roughley P, Hoemann C, DesRosiers E, Mwale F, Antoniou J, Alini M. The potential of chitosan-based gels containing intervertebral disc cells for nucleus pulposus supplementation. Biomaterials. 2006; 27(3):388–396. [PubMed: 16125220]

17. Smith LJ, Gorth DJ, Showalter BL, Chiaro JA, Beattie EE, Elliott DM, et al. In Vitro Characterization of a Stem Cell-Seeded Triple Interpenetrating Network Hydrogel for Functional Regeneration of the Nucleus Pulposus. Tissue Eng Part A. 2014; 20(13–14):1841–1849. [PubMed: 24410394]

18. Zeiter S, der Werf Mv, Ito K. The fate of bovine bone marrow stromal cells in hydrogels: a comparison to nucleus pulposus cells and articular chondrocytes. J Tissue Eng Regen Med. 2009; 3(4):310–320. [PubMed: 19319878]

19. Risbud MV, Albert TJ, Guttapalli AV, Edward JH, Alan SV, Alexander RS, et al. Differentiation of mesenchymal stem cells towards a nucleus pulposus-like phenotype in vitro: implications for cell-based transplantation therapy. Spine (Phila Pa 1976). 2004; 29(23):2627–2632. [PubMed: 15564911]

20. Kim IL, Mauck RL, Burdick JA. Hydrogel design for cartilage tissue engineering: A case study with hyaluronic acid. Biomaterials. 2011; 32(34):8771–8782. [PubMed: 21903262]

21. Burdick JA, Chung C, Jia X, Randolph MA, Langer R. Controlled degradation and mechanical behavior of photopolymerized hyaluronic acid networks. Biomacromolecules. 2005; 6(1):386–391. [PubMed: 15638543]

22. Chung C, Burdick JA. Influence of three-dimensional hyaluronic acid microenvironments on mesenchymal stem cell chondrogenesis. Tissue Eng Part A. 2009; 15:243–254. [PubMed: 19193129]

23. Chung C, Erickson IE, Mauck RL, Burdick JA. Differential Behavior of Auricular and Articular Chondrocytes in Hyaluronic Acid Hydrogels. Tissue Eng Part A. 2008; 14(7):1121–1131. [PubMed: 18407752]

24. Erickson IE, Kestle SR, Zellars KH, Farrell MJ, Kim M, Burdick JA, et al. High mesenchymal stem cell seeding densities in hyaluronic acid hydrogels produce engineered cartilage with native tissue properties. Acta Biomater. 2012; 8:3027–3034. [PubMed: 22546516]

25. Bian L, Guvendirena M, Mauck RL, Burdick JA. Hydrogels that mimic developmentally relevant matrix and N-cadherin interactions enhance MSC chondrogenesis. PNAS. 2013; 110(25):10117–10122. [PubMed: 23733927]

26. Collin EC, Grad S, Zeugolis DI, Vinatier CS, Clouet JR, Guicheux JJ, et al. An injectable vehicle for nucleus pulposus cell-based therapy. Biomaterials. 2011; 32(11):2862–2870. [PubMed: 21276612]

27. Park SH, Cho H, Gil ES, Mandal BB, Min BH, Kaplan DL. Silk-Fibrin/Hyaluronic Acid Composite Gels for Nucleus Pulposus Tissue Regeneration. Tissue Eng Part A. 2011; 17(23): 2999–3009. [PubMed: 21736446]

28. Peroglio M, Grad S, Mortisen D, Sprecher CM, Illien-Jünger S, Alini M, et al. Injectable thermoreversible hyaluronan-based hydrogels for nucleus pulposus cell encapsulation. Eur Spine J. 2012; 21(6):S839–S849. [PubMed: 21874295]

29. Jadin KD, Bae WC, Schumacher BL, Sah RL. Three-dimensional (3-D) imaging of chondrocytes in articular cartilage: growth-associated changes in cell organization. Biomaterials. 2007; 28(2): 230–239. [PubMed: 16999994]

30. Fisher MB, Henning EA, Söegaard NB, Dodge GR, Steinberg DR, Mauck RL. Maximizing cartilage formation and integration via a trajectory-based tissue engineering approach. Biomaterials. 2014; 35(7):2140–2148. [PubMed: 24314553]

31. Mauck RL, Soltz MA, Wang CC, Wong DD, Chao PHG, Valhmu WB. Functional tissue engineering of articular cartilage through dynamic loading of chondrocyte-seeded agarose gels. J Biomech Eng. 2000; 122:252–260. [PubMed: 10923293]

32. Huang AH, Yeger-McKeever M, Stein A, Mauck RL. Tensile properties of engineered cartilage formed from chondrocyte- and MSC-laden hydrogels. Osteoarthr Cartilage. 2008; 16(9):1074–1082.

33. Stegemann H, Stalder K. Determination of hydroxyproline. Clin Chim Acta. 1967; 18:267–273. [PubMed: 4864804]

34. Neuman RE, Logan MA. The determination of hydroxypoline. J Biol Chem. 1949:299–306. [PubMed: 18133395]
35. Huang AH, Farrell MJ, Mauck RL. Mechanics and mechanobiology of mesenchymal stem cell-based engineered cartilage. J Biomech. 2010; 43:128–136. [PubMed: 19828149]
36. Huang AH, Stein A, Tuan RS, Mauck RL. Transient exposure to transforming growth factor beta 3 improves the mechanical properties of mesenchymal stem cell-laden cartilage constructs in a density-dependent manner. Tissue Eng Part A. 2009; 15:3461–3472. [PubMed: 19432533]
37. Kluba T, Niemeyer T, Gaissmaier C, Gründer T. Human anulus fibrosis and nucleus pulposus cells of the intervertebral disc: effect of degeneration and culture system on cell phenotype. Spine. 2005; 30:2743–2748. [PubMed: 16371897]
38. Chen YC, Su WY, Yang SH, Gefen A, Lin FH. In situ forming hydrogels composed of oxidized high molecular weight hyaluronic acid and gelatin for nucleus pulposus regeneration. Acta Biomater. 2013; 9(2):5181–5193. [PubMed: 23041783]
39. Lefebvre V, Huang W, Harley VR, Goodfellow PN, Crombrugghe BD. SOX9 is a potent activator of the chondrocyte-specific enhancer of the pro alpha1(II) collagen gene. Mol Cell Biol. 1997; 17:2336–2346. [PubMed: 9121483]
40. Clouet J, Grimandi G, Pot-Vaucel M, Masson M, Fellah HB, Guigand L. Identification of phenotypic discriminating markers for intervertebral disc cells and articular chondrocytes. Rheumatology. 2009; 48:1447–1450. [PubMed: 19748963]
41. Lee CR, Sakai D, Nakai T, Toyama K, Mochida J, Alini M, et al. A phenotypic comparison of intervertebral disc and articular cartilage cells in the rat. Eur Spine J. 2007; 16:2174–2185. [PubMed: 17786487]
42. Rutges J, Creemers LB, Dhert W, Milz JS, Sakai D, Mochida J, et al. Variations in gene and protein expression in human nucleus pulposus in comparison with annulus fibrosus and cartilage cells: potential associations with aging and degeneration. Osteoarthr Cartilage. 2010; 18:416–423.
43. Minogue BM, Richardson SM, Zeef LA, Freemont AJ, Hoyland JA. Transcriptional profiling of bovine intervertebral disc cells: implications for identification of normal and degenerate human intervertebral disc cell phenotypes. Arthritis Res Ther. 2010; 12:R22. [PubMed: 20149220]
44. Minogue BM, Richardson SM, Zeef LA, Freemont AJ, Hoyland JA. Characterization of the human nucleus pulposus cell phenotype and evaluation of novel marker gene expression to define adult stem cell differentiation. Arthritis Rheum. 2010; 62:3695–3705. [PubMed: 20722018]
45. Stosiek P, Kasper M, Karsten U. Expression of cytokeratin and vimentin in nucleus pulposus cells. Differentiation. 1988; 39(1):78–81. [PubMed: 2469613]
46. Halloran DO, Grad S, Stoddart M, Dockery P, Alini M, Pandit AS. An injectable cross-linked scaffold for nucleus pulposus regeneration. Biomaterials. 2008; 29(4):438–447. [PubMed: 17959242]
47. Kuo SM, Wang YJ, Niu GC, Lu HE, Chang SJ. Influences of hyaluronan on type II collagen fibrillogenesis in vitro. J Mater Sci Mater Med. 2008; 19(3):1235–1241. [PubMed: 17701300]
48. Zhou S, Cui Z, Urban JP. Factors influencing the oxygen concentration gradient from the synovial surface of articular cartilage to the cartilage-bone interface: a modeling study. Arthritis Rheum. 2004; 50:3915–3924. [PubMed: 15593204]
49. Kobayashi S, Meir A, Urban J. Effect of cell density on the rate of glycosaminoglycan accumulation by disc and cartilage cells in vitro. J Orthop Res. 2008; 26(4):493–503. [PubMed: 17985391]
50. Temenoff JS, Shin H, Conway DE, Engel PS, Mikos AG. In vitro cytotoxicity of redox radical initiators for cross-linking of oligo(poly(ethylene glycol) fumarate) macromers. Biomacromolecules. 2003; 4(6):1605–1613. [PubMed: 14606886]
51. Martin JT, Milby AH, Chiaro JA, Kim DH, Hebela NM, Smith LJ, et al. Translation of an engineered nanofibrous disc-like angle-ply structure for intervertebral disc replacement in a small animal model. Acta Biomater. 2014; 10(6):2473–2481. [PubMed: 24560621]

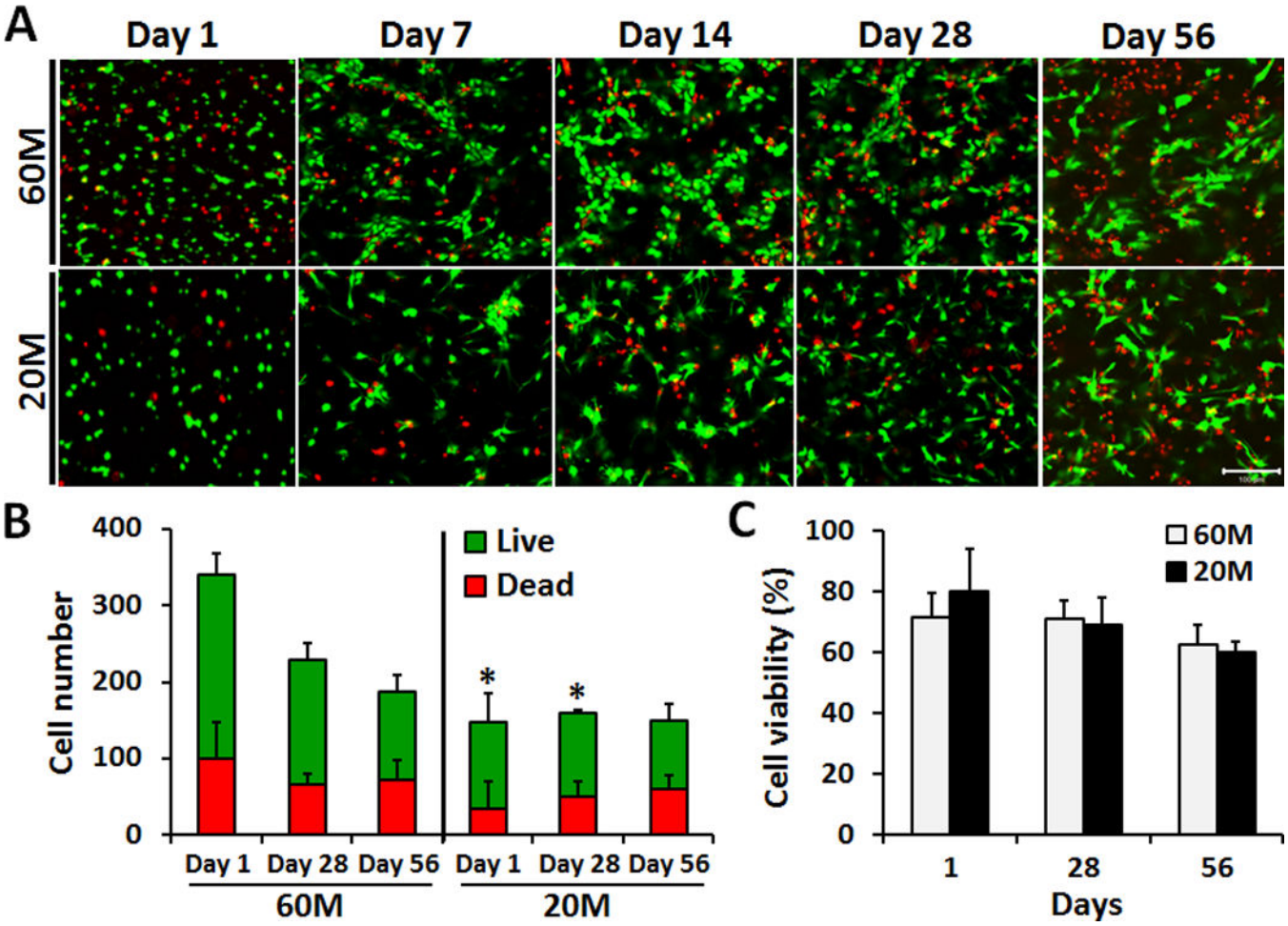

Fig. 1.

A) LIVE/DEAD staining of NPC-seeded HA constructs on days 1, 7, 14, 28 and 56 after encapsulation at either 60M or 20M seeding density (20× magnification, scale bar: 100 μm). B) Quantification of NPC number (live and dead) from images at days 1, 28 and 56. C) Quantification of NPC percent viability in HA constructs on days 1, 28 and 56.

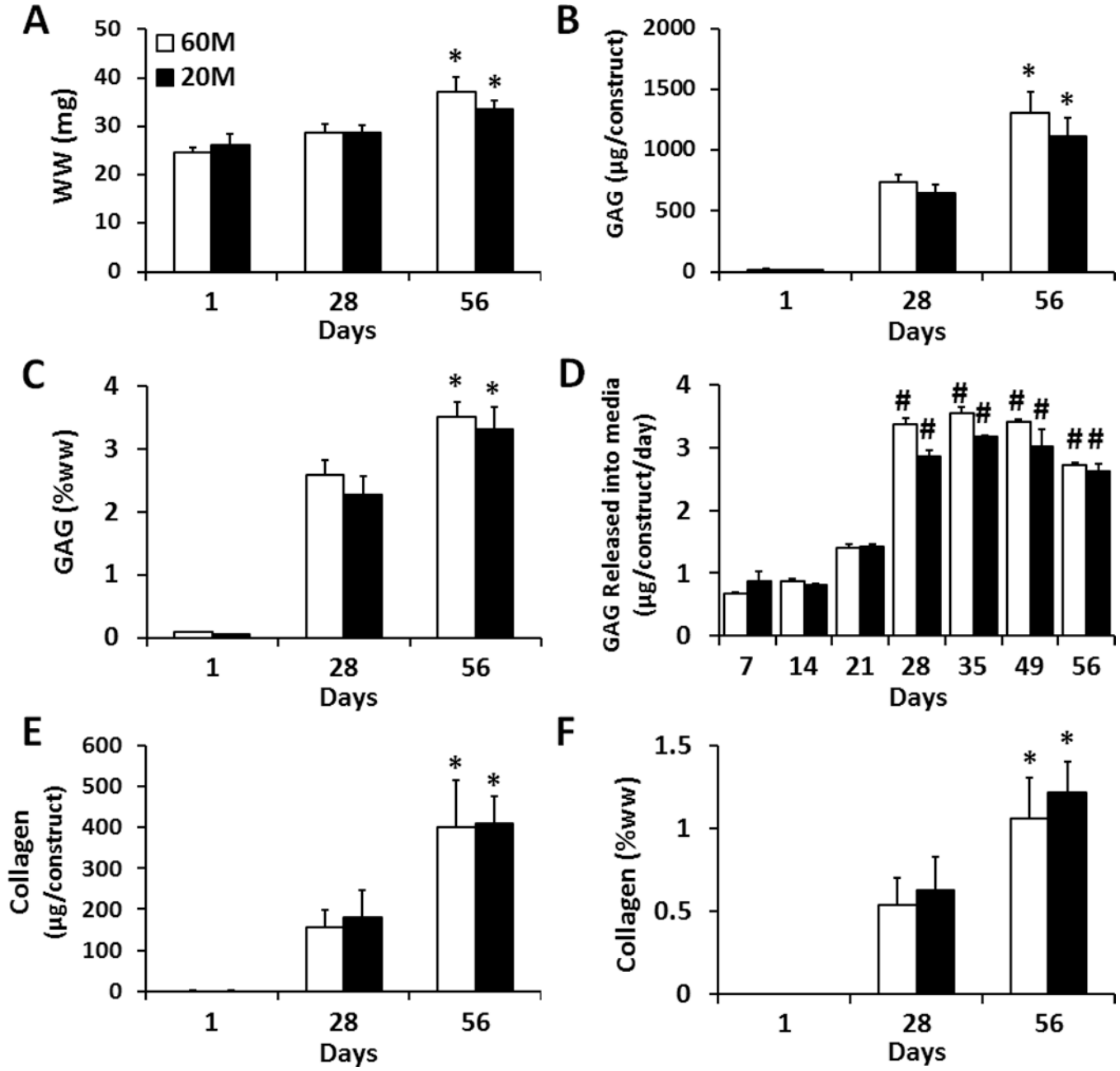

Fig. 2.

Biochemical composition of NP cell seeded HA constructs at seeding densities of 60M (white) and 20M (black) after 1, 28, 56 days of in vitro culture. A) Wet weight per construct, n=5. B) Total GAG content per construct, n=5. C) GAG content per wet weight, n=5. D) GAG released to the media (per construct per day), n=3. E) Collagen content per construct n=5. F) Collagen content per wet weight, n=5. (* indicates $p < 0.05$ vs. day 28 within same group; # indicates $p < 0.05$ vs. day 21 within same group)

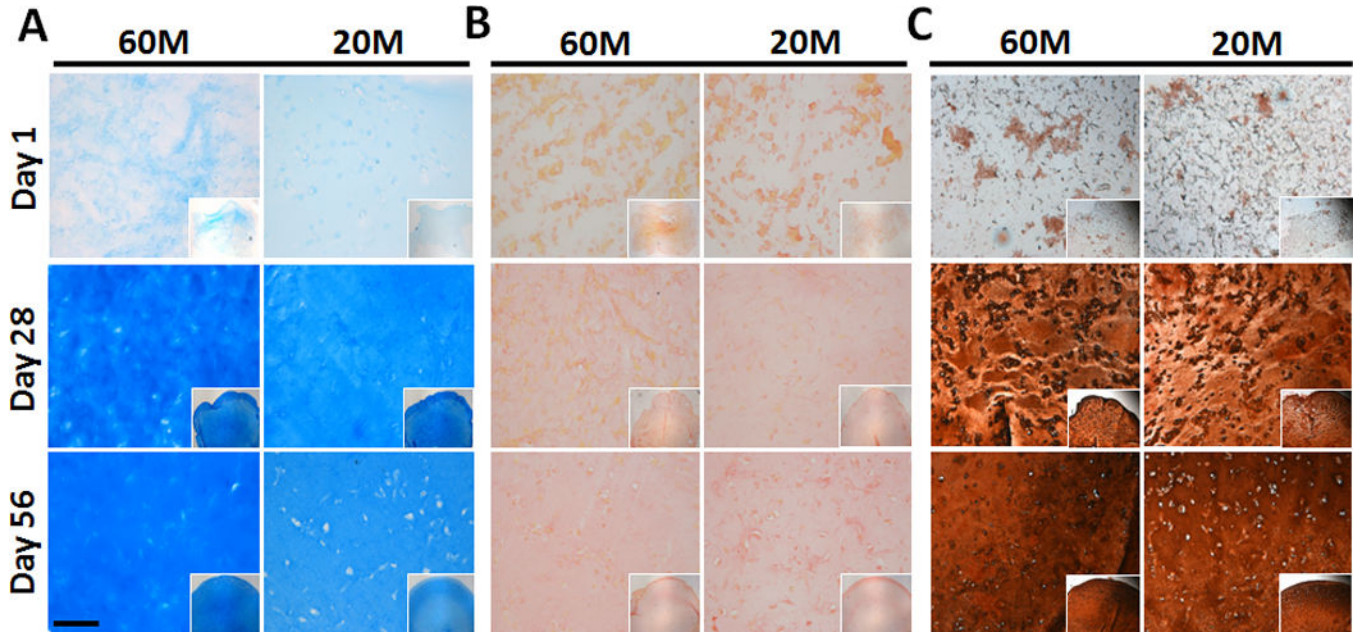

Fig. 3.

Matrix deposition in NPC-seeded HA constructs as a function of culture duration and seeding density. (A: Alcian blue staining of proteoglycans, B: Picrosirius red staining for collagens, C: immunostaining for collagen type II; 10× magnification (inset: 5×), scale bar: 100 μm).

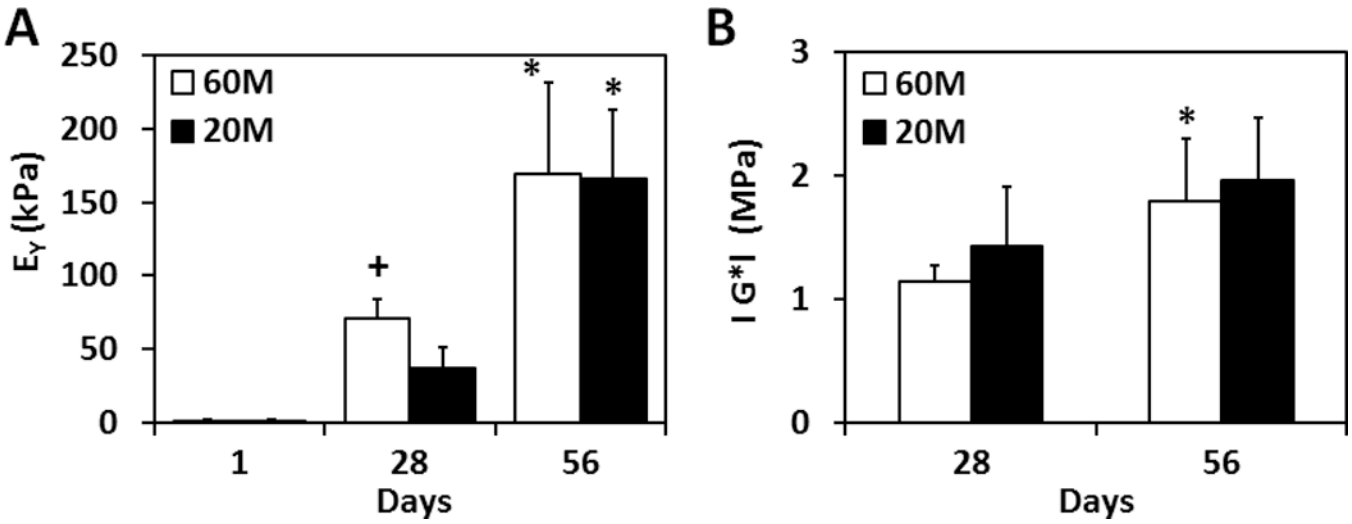

Fig. 4.

Equilibrium compressive modulus (A) and dynamic compressive modulus (B) of NPC-seeded HA constructs over 8 weeks of in vitro culture (*indicates $p < 0.05$ vs. at day 28; $^{+}$indicates $p < 0.05$ vs. 20M group, n=4~5/group/time point).

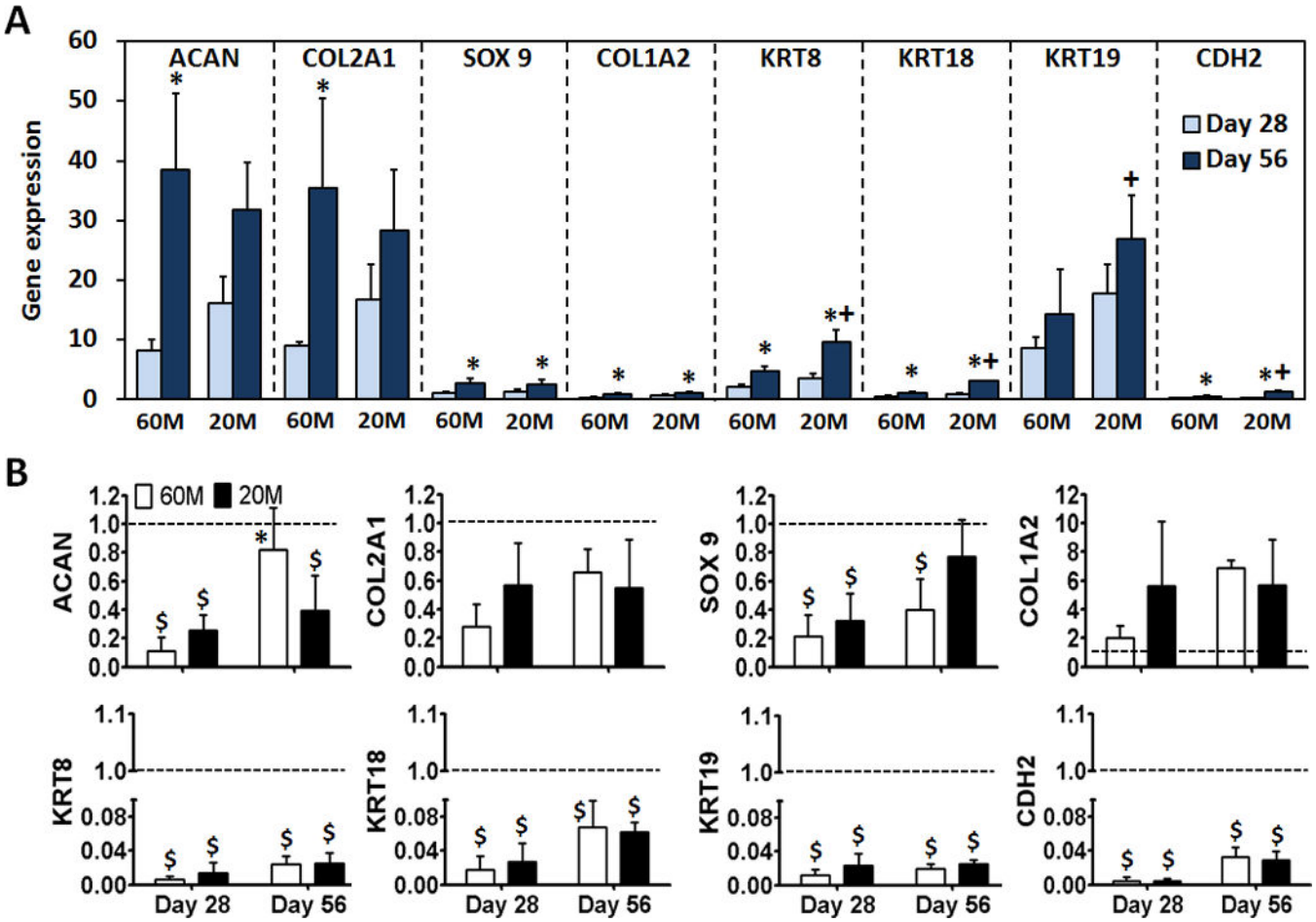

Fig. 5.

Expression of aggrecan (ACAN), collagen II (COL2A1), SOX 9, collagen I (COL1A2), cytokeratin (KRT) 8, 18, 19, and N-cadherin (CDH 2) after 28 and 56 day of culture for NPC-seeded HA constructs. A) Expression levels were normalized to glyceraldehyde 3-phosphate dehydrogenase (GAPDH) and expanded NP cells prior to encapsulation (* indicates $p < 0.05$ vs day 28 within same group; + indicates $p < 0.05$ vs 60M). B) Expression of the same genes in A) normalized to GAPDH and freshly isolated NP cells. Values are expressed as a ratio to fresh (dashed line) (* indicates $p < 0.05$ vs day 28 within same group; $ indicates $p < 0.05$ vs Fresh cells). (n=3/group/time point)

Table 1

PCR primer sequences

Primer	Accession Number	Forward primer	Reverse primer
ACAN	NM_173981.2	CCTGAACGACAAGACCATCGA	TGGCAAAGAAGTTGTCAGGCT
COL2A1	NM_001113224.1	AAGAAGGCTCTGCTCATCCAGG	TAGTCTTGCCCCACTTACCGGT
SOX9	XR_083993.1	TGAAGAAGGAGAGCGAGGAG	CTTGTTCTTGCTCGAGCCGTTGA
COL1A2	NM_174520.2	GGTAGCCATTTCCTTGGTGGTT	AATTCCAAGGCCAAGAAGCATG
KRT8	NM_001033610.1	ACCAGGAGCTCATGAATGTCAA	TCGCCCTCCAGCAGCTT
KRT18	XM_582930.4	TTGAGCTGCTCCATCTGCAT	AAGGCCAGCTTGGAGAACAG
KRT19	XM_875997.3	CGGTGCCACCATTGAGAACT	CAAACTTGGTGCGGAAGTCA
CDH2	XM_001250829.2	GCCATCAAGCCAGTTGGAA	TGCAGATCGAACCGGGTACT
GAPDH	NM_001034034.1	ATCAAGAAGGTGGTGAAGCAGG	TGAGTGTCGCTGTTGAAGTCG